Realization of Highly Reliable 10^{-20}-Level Instability Optical Phase Transmission over a 1402-Kilometer Commercial Fiber-Optic Network

Yang Xu(徐洋)[1,3,4†], Libo Li(李立波)[2†], Kan Zhao(赵侃)[2], Pingan Ma(马平安)[2], Zhiwei Zhang(张志伟)[2], Qi Shen(沈奇)[1,3,4], Faxi Chen(陈法喜)[2,4*], and Haifeng Jiang(姜海峰)[1,3,4]

[1]*Hefei National Research Center for Physical Sciences at the Microscale and School of Physical Sciences, University of Science and Technology of China, Hefei 230026, China*
[2]*Jinan Institute of Quantum Technology, Jinan 250101, China*
[3]*Shanghai Research Center for Quantum Science and Chinese Academy of Sciences Center for Excellence in Quantum Information and Quantum Physics, University of Science and Technology of China, Shanghai 201315, China*
[4]*Hefei National Laboratory, University of Science and Technology of China, Hefei 230088, China*

(Received 1 August 2025; accepted manuscript online 3 December 2025)

Optical phase transfer via fiber optics is the most effective method for optical frequency standard comparison on the scale below thousands of kilometers. However, the monotonic phase discrimination range of conventional optical phase-locked loops is limited, and link delays restrict the control bandwidth, which makes it a challenge to achieve a continuously reliable optical link. This paper presents an event-timing-based phase detection method that overcomes the monotonic phase discrimination range limitation of conventional phase-locked loops through dual-edge timestamp recording, achieving an optical phase measurement resolution on the order of 10 attoseconds. With such a technique, we established a 7-segment-cascaded optical link over 1402 km of commercial fiber while sharing dense wavelength division multiplexing (DWDM) channels with live telecom traffic. The system maintained continuous operation for 11.7 days without phase cycle slips despite encountering 15 km aerial fiber noise up to 21000 $\mathrm{rad^2\cdot Hz^{-1}\cdot km^{-1}}$ at 1 Hz. Relative instabilities of the link are 3.7×10^{-15} at 1 s and 3.9×10^{-20} at 100000 s.

DOI: 10.1088/0256-307X/42/12/120401 CSTR: 32039.14.0256-307X.42.12.120401

1. Introduction. Ultra-high-stability optical frequency transfer plays a pivotal role in time-frequency metrology,[1–4] quantum communication,[5–8] and fundamental physics research.[9,10] This technology typically employs a large-scale unequal-arm Michelson interferometer, where the short arm acts as a low-noise reference path, while the long arm incorporates an optical fiber link to transmit the frequency signal.[11,12] By heterodyne beating the round-trip signal from the fiber arm with the reference signal from the short arm, phase noise and path-length variations are detected and actively compensated, forming a delayed optical phase-locked loop system.

To address fiber attenuation (∼0.2 dB/km), bidirectional Erbium-doped fiber amplifiers (EDFAs) are widely adopted.[13] However, cascaded EDFAs progressively amplify amplified spontaneous emission (ASE) noise, degrading the signal-to-noise ratio (SNR) and risking self-oscillation. Although fiber Brillouin amplifiers provide lower noise amplification,[1,14–16] their reliance on dedicated fibers limits practical deployment. Consequently, bidirectional EDFAs dominate long-haul fiber links despite their noise limitations. Accumulated ASE and distance-dependent environmental noise further constrain the noise suppression capability of single-span architectures, necessitating segmentation of long links into cascaded shorter segments.[13] Leveraging these approaches, nations including Europe (e.g., REFIMEVE+[17]), the United States,[18] Japan,[19] and China[20] have established continental-scale optical frequency transfer networks.

Nevertheless, previous optical links experience phase cycle slips from time to time due to their limited monotonic phase discrimination range (usually below 2π radian) and bandwidth restrictions imposed by fiber delay (see Table 1). Although one can increase the phase dynamic range by frequency dividing the heterodyne signal before phase detection,[11,12] it is difficult to make the frequency division ratio sufficiently large to ensure the control bandwidth and phase detection resolution. These limitations make the systems vulnerable to cycle slips under high environmental noise, particularly in urban areas where fiber networks experience elevated noise levels. For instance, aerial fiber segments disrupted by environmental factors such as traffic-induced vibrations and thermal fluctuations encounter noise levels exceeding 1000 $\mathrm{rad^2\cdot Hz^{-1}\cdot km^{-1}}$ at 1 Hz,[21,22] inevitably leading to phase tracking errors.

This work presents an optical phase detection technique based on digital event timing, enabling high-resolution phase tracking and a large monotonic phase

†These authors contributed equally to this work.
*Corresponding author. Email: chenfaxi@jiqt.org
© 2025 Chinese Physical Society and IOP Publishing Ltd. All rights, including for text and data mining, AI training, and similar technologies, are reserved.

Table 1. Performance of international fiber links for long-haul optical phase transfer.

System (country)	Length (km)	Duration (days)	Noise ($rad^2 \cdot Hz^{-1} \cdot km^{-1}$ at 1 Hz)	Cycle slips
MPQ-PTB-MPQ (Germany) [1,15]	920	3	0.11	4 instances
Villetaneuse-Nancy-Villetaneuse (France) [23]	1100	3.5	100	73 instances
INRIM-LENS-INRIM (Italy) [24]	1284	<1	22	>20 instances
UTokyo-NTT-UTokyo (Japan) [22]	240	<1	1100	0.4%
This work (China)	1402	11.7	60–21000	0

discrimination range. This approach ensures robust phase tracking with reliability in the presence of high environmental noise, even when phase variations exceed 10000π radians within a millisecond, without causing the phase-locked loop to be out of lock. Validated on a 1402 km commercial fiber network incorporating 15 km of aerial fibers, the system achieved highly stable optical frequency transfer under extreme noise conditions. Continuous operation over 11 days without cycle slips demonstrated its robustness; the relative instabilities are about 3.7×10^{-15} at 1 s, 3.9×10^{-20} at 100000 s, and 4.9×10^{-20} at 200000 s.

2. Experimental Setups. The 1402 km bidirectional fiber link, as depicted in Fig. 1, comprises two parallel single-mode fibers within a shared commercial cable, connecting Wuhan (30.53969°N, 114.34771°E) to Chuzhou (32.01207°N, 117.94809°E). Both the starting point and endpoint of the link are situated in Chuzhou. The reference optical signal is provided by a laser with a sub-Hz linewidth operating at a wavelength of 1550.12 nm. The optical phase transfer performance is measured using a dead-time-free counter. The optical fibers used are not dedicated; instead, We employ channel #34 of the dense wavelength division multiplexing (DWDM) to achieve long-distance optical frequency transmission without interfering with other communication services on different channels of the link.

The length and loss of the link are shown in Table 2. The total optical link loss exceeds 450 dB, with an average attenuation greater than 0.32 dB/km. To compensate for significant attenuation, a total of 22 remotely controllable bi-directional EDFAs have been installed at the nodes, each providing approximately 10–25 dB gain in both directions. Optical filters with a 25 GHz bandwidth are inserted before and after each pump to suppress wavelengths outside the EDFA's operational range, preventing noise from entering and destabilizing the amplifier.

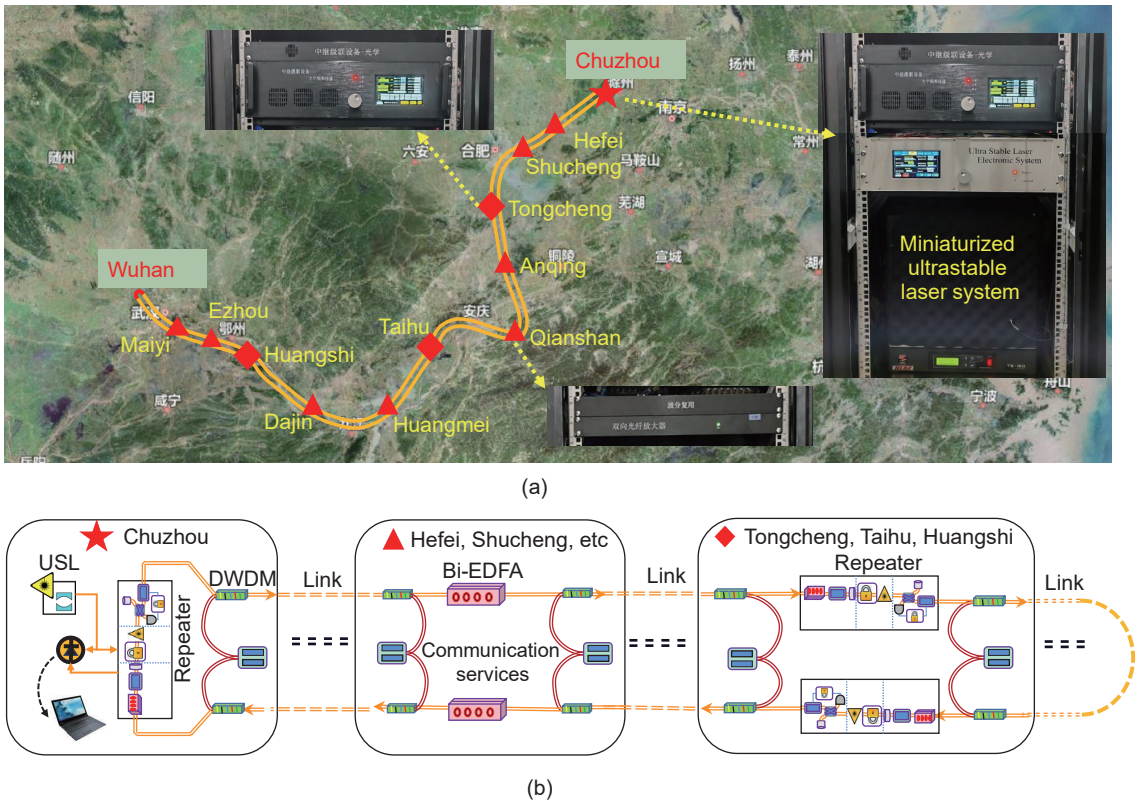

Fig. 1. Experimental System. (a) Satellite image showing the cascaded ultra-stable optical frequency transfer experiment, which employs field-deployed fibers between Chuzhou and Wuhan. Map data: Google, CNES/Astrium, DigitalGlobe. The entire optical link comprises a pair of 701-km-long telecom fibers (housed in the same cable duct) that traverse 13 metropolitan areas. Six repeaters are installed in Tongcheng, Taihu, and Huangshi to extend the control bandwidth. (b) Schematic of the node experimental setup and link configuration. Abbreviations: USL, ultra-stable Laser; DWDM, dense wavelength division multiplexer; Bi-EDFA: bidirectional Erbium-doped fiber amplifier.

Table 2. Length and attenuation of optical fibers.

Segment	Length (km)	Attenuation (dB)	
		Fiber A	Fiber B
Chuzhou–Hefei	81.8	27.5	28.8
Hefei–Shucheng	64.5	21.3	19.1
Shucheng–Tongcheng	59.7	18.9	20.9
Tongcheng–Anqing	84.1	25.5	24.7
Anqing–Qianshan	55.5	15.9	17.8
Qianshan–Taihu	54.2	19.3	17.5
Taihu–Huangmei	76.4	22.1	24.5
Huangmei–Dajin	36.0	14.1	12.8
Dajin–Huangshi	73.8	20.1	21.1
Huangshi–Ezhou	22.5	9.8	8.7
Ezhou–Maiyi	66.5	20.1	23.7
Maiyi–Wuhan	26.2	11.0	12.6

The fundamental limitation of the delayed phase-locked loop is that it has a maximum control bandwidth of $1/(4\tau)$, where τ is the delay. To enhance phase noise compensation in long-distance, high-noise fiber links, a multi-segment compensation approach is usually employed.[13] Here, six placed repeaters in Tongcheng, Taihu, and Huangshi divide the 1402 km link into seven segments, each limited to 230 km, improving noise suppression.

The infrastructure includes 15 km of aerial fiber with exceptionally high phase noise levels (60–21000 $\mathrm{rad^2\cdot Hz^{-1}\cdot km^{-1}}$ at 1 Hz), exceeding international benchmarks by up to three orders of magnitude (Table 1). Transient environmental perturbations induce optical phase variations exceeding 10000π radians within 1 ms detection intervals, even in shorter segments. These extreme fluctuations surpass the operational limits of conventional phase detection methods, including high-division-ratio analog phase detectors[23,27] and digital phase measurement systems.[22,28] Thus, expanding the unambiguous detection window is required for maintaining phase coherence in these fiber networks.

As shown in Fig. 2, the repeater consists of three modules: the receiving module, the local laser locking module, and the transmitting module. It is designed to meet the requirements for on-site installation and long-term operation in a communication equipment room. The optical components are housed in a 1U 19-inch chassis, while the electronic components are housed in a 3U chassis. The receiving module incorporates a −40 MHz frequency-shifted acousto-optic modulator (AOM2) and a half-pass Faraday mirror (HFM). Together with the transmitting module of the preceding stage, the receiving module forms a large-delay optical phase-locked loop that compensates for fiber noise. The primary function of the local laser locking module is to lock a kilo-Hertz linewidth fiber laser to the received laser signal from the preceding stage. With a control bandwidth of 20–50 kHz provided by the electronic servo, the locked laser output precisely replicates the signal from the preceding stage, ensuring that the output laser signal maintains a high SNR for reliable transmission to the next station. The transmitting module consists of a 50/50 beam-splitting Michelson interferometer with asymmetric arm lengths. The short arm, which has negligible length and phase noise, is connected to a Faraday mirror (FM), while the long arm transmits the optical signal to the next station. An acousto-optic modulator (AOM1) with a +50 MHz frequency shift is inserted to compensate for phase noise while the laser signal is transmitted to the next station over the long arm.

The noise cancellation system includes sections of optical single-pass fibers, which inevitably affect long-term stability and accuracy due to temperature drift. To mitigate these effects, the length of optical fibers between components is limited to 10 cm, with the length difference between fibers in the interference optical path kept below 1 cm. Additionally, by precisely controlling the temperature of the optical module within the repeater, temperature fluctuations are restricted to a standard deviation of 10 mK. These approaches minimize the impact of short,

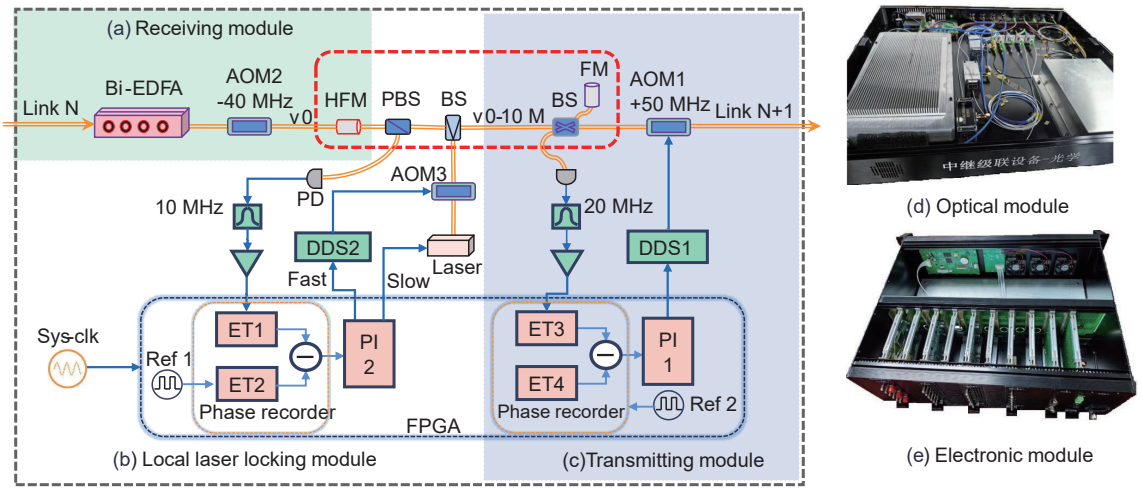

(d) Optical module

(e) Electronic module

Fig. 2. Repeater configuration schematics and physical photos. (a) Receiving module; (b) Local laser locking module; (c) Transmitting module; (d) Physical photo of the optical module; (e) Physical photo of the electronic module. Abbreviations: AOM, acousto-optic modulator; Bi-EDFA, bidirectional Erbium-doped fiber amplifier; HFM, half-pass Faraday mirror; PBS, polarizing beam splitter; BS, beam splitter; FM, Faraday mirror; PD, photodetector; DDS, direct digital synthesis (signal generator); ET, event timer; PI, digital proportional-integral controller; Sys-clk, system clock; Ref, reference frequency.

uncompensated extra-loop fibers from the repeater stations, contributing to a time instability of below 0.05 fs/K.

Moreover, substantial environmental noise induces rapid polarization fluctuations in the transmission signal, which alter the power of the beat signal between the signal laser and the local laser. To ensure proper alignment of polarization states in the interferometric signals received at each repeater station, a polarizing beam splitter (PBS) is used to generate two optical beating signals.[29] A signal with a high SNR is then automatically selected for phase locking.

A phase detection module (phase recorder) based on event timing is designed to expand the monotonic phase discrimination range of phase detection. It uses two synchronous event timers (ETs) to record the rising edges of the reference frequency and the interference heterodyne signal to be tested, with the system clock as the timing reference. The ETs exhibit a temporal resolution of approximately 100 ps using the delay chain units inside the FPGA,[30,31] which corresponds to an optical phase measurement resolution in the 10 as order of magnitude. The time difference between these signals serves as error information, significantly increasing the monotonic phase discrimination range. Currently, the method is limited by the RF bandpass filter bandwidth (∼6 MHz). The error information is processed by a digital PI controller (PI1), which adjusts the direct digital synthesizer (DDS1) to drive the acousto-optic modulator (AOM1) for noise compensation. All digital measurements and controls are implemented using a Xilinx Spartan-6 series FPGA.

3. Experimental Results. Figure 3 shows the phase noise power spectral density (PSD) of free-running and compensated optical links. Overhead optical fibers are susceptible to human activities, and there are significant differences in noise intensity at different times. Statistical analysis shows that there are two kinds of noise distribution: high intensity and medium intensity. The phase fluctuation remains moderate in about 90% of the operation time but rises sharply in 5%–10% of the time interval due to transient environmental factors. The free-running link exhibits a phase jitter dynamic range (1–10 kHz) spanning 270–2400 rad; the implementation of an optical phase-locked loop suppresses this jitter to below 100 rad.

As shown in Fig. 4, within a continuous recording period of 11.7 days, the peak-to-peak variation in the link's transmission delay is approximately 165 ns, corresponding to an average fiber-optic temperature change of 3 ℃. The short-term fluctuation of the out-of-loop phase is about 3 fs, the daily fluctuation is about 30 fs, and the long-term drift is less than 60 fs. During this period, ambient temperature fluctuations generally exceeded 10 ℃. Since most of the fiber-optic cables are buried underground, the temperature change of the fibers is reduced to approximately one-third or one-fourth of that in exposed environments. The moderate rain on October 6–7 basically corresponded to the high-noise period of the link. We believe that the compensated link optical phase drift mainly originates from

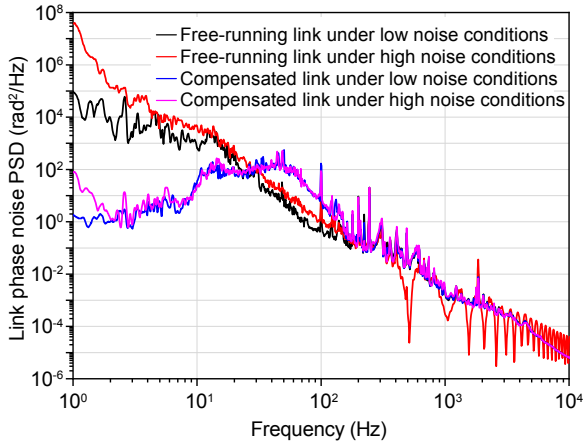

Fig. 3. Power spectral density of the link phase noise: the red (free-running link) and magenta (compensated link) curves correspond to measurements of the free-running and compensated links, respectively, under high link noise conditions; the black (free-running link) and blue (compensated link) curves correspond to those under low link noise conditions.

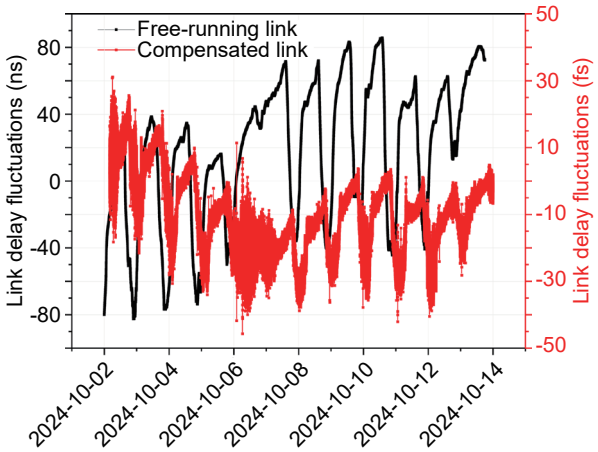

Fig. 4. Link delay fluctuations: the black curve (free-running link) and red curve (compensated link) correspond to the delay fluctuations of the free-running and compensated links, respectively, measured under the condition of a one-second gate time with no data excluded.

polarization mode dispersion of fibers[18,32] and is also influenced by the frequency asymmetry between forward and backward propagation signals in the closed loop.

Figure 5 hows that the compensated link instability values are 3.7×10^{-15} at 1 s, 3.9×10^{-20} at 100000 s, and 4.9×10^{-20} at 200000 s. The free-running link instability values, which were obtained by calculating the recorded real-time phase compensation amount, are 3.1×10^{-12} at 1 s, 2.2×10^{-13} at 100000 s, and 9.2×10^{-14} at 200000 s. The instability of the 1400 km free-running link between Braunschweig (Germany) and Strasbourg (France)[14] is shown by the green dotted curve, at a level approximately two orders of magnitude below that of our cases.

The demonstrated 3.9×10^{-20} instability at 100000 s is sufficient for testing gravitational redshift predictions in Einstein's equivalence principle.[9] The event-timing phase detection paradigm could be extended to microwave-frequency transfer systems,[33] particularly for

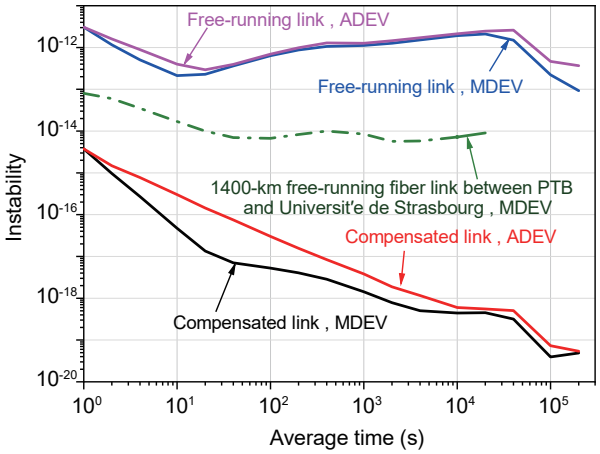

Fig. 5. Instability of the optical link: the magenta curve (free-running link, ADEV), blue curve (free-running link, MDEV), red curve (compensated link, ADEV), and black curve (compensated link, MDEV) correspond to the instability measurements of the respective optical links (ADEV: Allan Deviation; MDEV: Modified Allan Deviation); the green dotted curve corresponds to the instability of a 1400-km free-running link between Braunschweig (Germany) and Strasbourg (France). [14]

next-generation very long baseline interferometry (VLBI) networks requiring $<10^{-16}$ long-term stability.

4. Summary. We have demonstrated robust ultra-stable optical phase transfer across a 1402 km operational telecommunication fiber network, achieving uninterrupted operation for 11.7 days without any phase cycle slips while maintaining full compatibility with coexisting DWDM channels. The system's success under extreme environmental conditions—where the uncompensated link exhibits phase noise power spectral densities ranging from 60 to 21000 $\mathrm{rad^2{\cdot}Hz^{-1}{\cdot}km^{-1}}$ at 1 Hz—exceeds typical international infrastructure by up to three orders of magnitude, thereby establishing new benchmarks for resilient frequency dissemination. The relative instability of the link is 3.7×10^{-15} at 1 s, 3.9×10^{-20} at 100000 s, and 4.9×10^{-20} at 200000 s. This research serves as a crucial bridge between laboratory-scale advancements in optical clocks and the development of practical field-deployable quantum infrastructure. It may contribute to the ongoing effort to redefine SI units through the establishment of globally accessible optical frequency standards.

Acknowledgements. This work was supported by the National Key Research and Development Program of China (Grant No. 2020YFC2200103), the Shandong Provincial Natural Science Foundation (Grant Nos. ZR2022LLZ006 and ZR2022LLZ011), the Innovation Program for Quantum Science and Technology (Grant Nos. 2021ZD0300904 and 2021ZD0300903), and the Key R&D Plan of Shandong Province (Grant No. 2023CXPT105).

References

[1] Predehl K, Grosche G, Raupach S M F, Droste S, Terra O, Alnis J, Legero T, Hänsch T W, Udem T, Holzwarth R, and Schnatz H 2012 *Science* **336** 441
[2] Beloy K, Bodine M I, Bothwell T, and Brewer S M 2021 *Nature* **591** 564
[3] Schioppo M, Kronjäger J, Silva A *et al.* 2022 *Nat. Commun.* **13** 212
[4] Dimarcq N, Gertsvolf M, Mileti G *et al.* 2024 *Metrologia* **61** 012001
[5] Chen J P, Zhang C, Liu Y *et al.* 2020 *Phys. Rev. Lett.* **124** 070501
[6] Yu Y, Ma F, Luo X Y *et al.* 2020 *Nature* **578** 240
[7] Clivati C, Meda A, Donadello S *et al.* 2022 *Nat. Commun.* **13** 157
[8] Pompili M, Hermans S L, Baier S *et al.* 2021 *Science* **372** 259
[9] Delva P, Lodewyck J, Bilicki S *et al.* 2017 *Phys. Rev. Lett.* **118** 221102
[10] Roberts B M, Delva P, Al-Masoudi A *et al.* 2020 *New J. Phys.* **22** 093010
[11] Ma L S, Jungner P, Ye J, and Hall J L 1994 *Opt. Lett.* **19** 1777
[12] Jiang H, Kéfélian F, Crane S *et al.* 2008 *JOSA B* **25** 2029
[13] Lopez O, Haboucha A, Chanteau B *et al.* 2012 *Opt. Express* **20** 23518
[14] Raupach S M, Koczwara A, and Grosche G 2015 *Phys. Rev. A* **92** 021801
[15] Droste S, Ozimek F, Udem T *et al.* 2013 *Phys. Rev. Lett.* **111** 110801
[16] Koke S, Kuhl A, Waterholter T *et al.* 2019 *New J. Phys.* **21** 123017
[17] Vojtech J, Smotlacha V, Šlapák M *et al.* 2020 *Proceedings Volume 11502, Infrared Remote Sensing and Instrumentation XXVIII* 115020N
[18] Williams P A M, Swann W C, and Newbury N R 2008 *J. Opt. Soc. Am. B* **25** 1284
[19] Musha M, Hong F L, Nakagawa K, and Ueda K 2008 *Opt. Express* **16** 16459
[20] Deng X, Zhang X, Zang Q *et al.* 2024 *Chin. Phys. B* **33** 020602
[21] Fujieda M, Kumagai M, and Nagano S 2010 *IEEE T. Ultrason Ferr.* **57** 168
[22] Akatsuka T, Goh T, Imai H *et al.* 2020 *Opt. Express* **28** 9186
[23] Chiodo N, Quintin N, Stefani F *et al.* 2015 *Opt. express* **23** 33927
[24] Calonico D, Bertacco E, Calosso C *et al.* 2014 *Appl. Phys. B* **117** 979
[25] Deng X, Liu J, Zang Q *et al.* 2018 *Appl. Opt.* **57** 9620
[26] Wang D, Liu J, Jiao D D *et al.* 2024 *Opt. Fiber Technol.* **87** 103923
[27] Lopez O, Haboucha A, Kéfélian F *et al.* 2010 *Opt. Express* **18** 16849
[28] Hu L, Xue R, Wu G, and Chen J 2021 *Rev. Sci. Instrum.* **92** 053709
[29] Cecilia C, Savio P, Abrate S *et al.* 2020 *Opt. Express* **28** 8494
[30] Mattada M and Guhilot H 2022 *J. King Saud Univ* **34** 418
[31] Song Z P, Zhao Z X, Yu H S *et al.* 2020 *Sensors* **20** 2172
[32] Xu D, Lopez O, Amy-Klein A *et al.* 2021 *Opt. Express* **29** 17476
[33] Pound R 1946 *Rev. Sci. Instrum.* **17** 490